Synchronization, phase locking, and metachronal wave formation in ciliary chains

Thomas Niedermayer, Bruno Eckhardt, and Peter Lenz
Fachbereich Physik, Philipps-Universität Marburg, 35032 Marburg, Germany

(Received 15 February 2008; accepted 16 June 2008; published online 22 September 2008)

Synchronization and wave formation in one-dimensional ciliary arrays are studied analytically and numerically. We develop a simple model for ciliary motion that is complex enough to describe well the behavior of beating cilia but simple enough to study collective effects analytically. Beating cilia are described as phase oscillators moving on circular trajectories with a variable radius. This radial degree of freedom turns out to be essential for the occurrence of hydrodynamically induced synchronization of ciliary beating between neighboring cilia. The transitions to the synchronized and phase-locked state of two cilia and the formation of metachronal waves in ciliary chains with different boundary conditions are discussed. © *2008 American Institute of Physics*.
[DOI: 10.1063/1.2956984]

Many microorganisms use cilia, little hairlike projections on their surfaces, for swimming and feeding. Cilia have a characteristic pattern of motion by which they can put fluid into motion at low Reynolds numbers. They often occur in arrays and show highly coordinated motion, where neighboring cilia beat cooperatively in a synchronized fashion or maintain a constant phase difference as in the case of metachronal waves. We focus here on the case of monocilia, where the appendages execute a circular motion, and develop a simple phase oscillator model for the synchronization phenomena. Neighboring cilia influence each other via the velocity fields induced in the surrounding fluid. The hydrodynamic interactions are shown to result in collective effects, provided the cilia possess some flexibility in their motion, as is the case for the slightly varying radius of their trajectory as discussed here. The model derived here is simpler than previous models, allows for an analytic analysis, and highlights the significance of some flexibility in ciliary motion. By coupling several cilia in a linear chain, we obtain a phase oscillator model for metachronal waves.

I. INTRODUCTION

Cyclical processes are ubiquitous in living matter.[1] Important examples include the movement of body parts for locomotion, the beating of a heart, or metabolic processes. Many of these biological cycles need adequate timing. In principle, this timing could be organized in a passive way from a central unit via, e.g., neuronal or biochemical pathways. But in many cases, there is no such central control unit, the units are timed individually and independently, and timing arises from synchronization by suitable couplings.[2]

Prominent examples for such synchronization processes in nature are the adjustment of the glowing rhythms of huge colonies of fireflies,[3] the synchronized firing of pacemaker neurons,[4] or coordinated calcium oscillations in neighboring muscle cells.[5] The human circadian clock is externally synchronized, namely by the perpetual change of daylight.[6] The stepping of people on flexible bridges can be synchronized by a coupling between human stepping and the response of the bridge.[7,8]

The qualitative understanding of "synchronization" as an adaption of the rhythms of self-sustained oscillators has been quantified and formalized in many ways.[9,10] For the phase oscillators $\varphi_i(t)$ discussed here, we will use the definitions given in Ref. 11. In a *synchronized* state all N oscillators have identical phases, i.e., $\varphi_i(t)=\varphi_j(t)$ for $i,j=1,\ldots,N$. A *phase-locked* state has identical phase velocities, i.e., $\dot{\varphi}_i(t)=\dot{\varphi}_j(t)$. And finally, an *entrained* state has identical mean phase velocities: $\tilde{\omega}_i=\tilde{\omega}_j$, where $\tilde{\omega}_i \equiv \lim_{t\to\infty}[\varphi_i(t)-\varphi(0)]/t$.[51] The case of a phase-locked state with constant phase differences between the oscillators and a nonvanishing mean velocity, which in dynamical systems terms corresponds to a traveling wave, is known in the biological literature on cilia[12] as a *metachronal* wave: $\varphi_{i+1}(t)=\varphi_i+\psi$ (and of course $\dot{\varphi}_i \neq 0$).

In this paper, we discuss the occurrence of synchronization phenomena in ciliary systems. Cilia are hairlike projections covering many small organisms. They are used to produce fluid flow in the surrounding environment for transport or cellular motion. Cilia also play an important role in the human body by creating air currents for transport out of the human lungs. There is also experimental evidence that during development, cilia-generated flow contributes to the placement of our organs.[13,14]

Most cilia are built out of nine sets of microtubule doublets surrounding a pair of single microtubules in the center.[15] Dynein motors cause bending deformations, giving rise to characteristic beating patterns typically consisting of a power and a recovery stroke.[12] Other cilia (monocilia that lack the central pair of microtubules[13,16]) perform a rapid rotational motion[17] and very often are tilted, giving rise to nonsymmetrical velocity fields.

In many cases, cilia are uniformly aligned in rows[18] and beat in a coordinated fashion in either complete synchrony or by maintaining a constant phase difference between oscillators, thus creating a metachronal wave.[19] Metachronal waves

can propagate in the direction of the effective stroke (symplectic metachronal waves), in the opposite direction (antiplectic), perpendicular direction (laeoplectic or dexioplecit), or oblique direction.[20]

Small animals, such as *Paramecium*, use this collective ciliary motion to swim. Typically, the cilia beat with a traveling helical wave, where the direction of the ciliary effective stroke is oblique to the long axis of the body.[19] Thus, a *Paramecium* swims in a spiral course, rotating around its longitudinal axis. By changing the axis of the helix, a *Paramecium* can steer and reverse its direction of motion.[21] This swimming is extremely efficient: The ~100 μm long *Paramecium* can swim with a velocity of the order of ~1 mm/s.

The causes for this cooperative behavior in ciliary arrays are unclear. Of course, motion could be triggered biochemically[22] but there are also experimental indications that hydrodynamic interactions couple the beating pattern of neighboring cilia.[23] We show here analytically that hydrodynamic interactions can indeed lead to collective ciliary motion, in particular to synchronization of beating and to metachronal wave formation. We build on a previous model[24] that also introduced a phase oscillator description in the spirit of the "discrete cilia models" introduced by Blake.[25,26] Each cilium is treated separately, and the total velocity field in the system is given by the superposition of the velocity fields induced by each cilium, as discussed in Sec. II. The new model introduced here is complex enough to capture the essential properties of the flow a beating cilium induces in the surrounding fluid and to show synchronization and phase locking between neighboring cilia and metachronal wave formation. At the same time, it is simple enough to make the phenomena analytically accessible.

The phase oscillator model introduced in Ref. 24 did not show synchronization. The important generalization introduced here is the inclusion of an additional degree of freedom in ciliary motion that allows for some variability in the trajectory. As we show here, this additional degree of flexibility is sufficient to lead to the mentioned collective effects. Thus, the model introduced here bridges the gap between simple models not showing collective effects (such as the one introduced in Ref. 24) and more complex numerical simulations where these phenomena have been observed; see, e.g., Refs. 27–29. In particular, for two interacting cilia our model shows the same synchronization properties as a more complicated model of interacting helices.[30]

Our equations of motion for a chain of hydrodynamically coupled cilia are reminiscent of the Kuramoto model.[11,31,32] However, our equations differ in two features from Kuramoto's model: (i) The oscillators are only coupled to their nearest neighbors, and (ii) the coupling function is not sinusoidal. Both modifications have been considered before. In Refs. 33–35, the interactions are restricted to nearest neighbors, and it was shown that only finite chains or subsets can phase-lock. More general coupling functions were considered in Refs. 36 and 37, and the combined effect in Refs. 38 and 39. As we will see below, the specific interactions induced by the hydrodynamic coupling have different properties, so that the results from these studies are not immediately applicable.

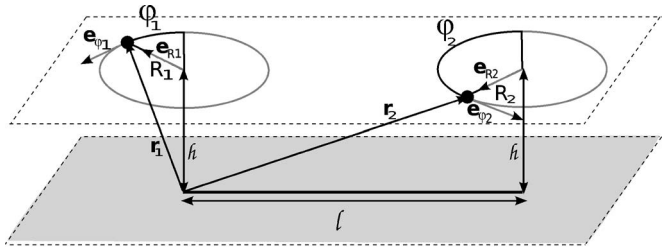

FIG. 1. Cilia are modeled as Stokeslets moving along (nearly) circular trajectories perpendicular to the membrane the cilia are attached to. Neighboring cilia interact via their induced velocity fields. For sufficiently low ciliary densities, the hydrodynamic interactions are weak and only lead to small variations in the radius of the trajectory.

The outline of this paper is as follows: First, the theoretical description of a beating single cilium is introduced (Sec. II). The description of hydrodynamic interactions for two interacting cilia and the derivation of the fundamental model are discussed in Sec. III. The transition to a phase-locked or synchronized state is discussed in Sec. IV. In Sec. V, we analyze these phenomena (and metachronal wave formation) in ciliary arrays. We conclude with a summary and an outlook in Sec. VI.

II. BEATING OF A SINGLE CILIUM

To study collective effects in ciliary arrays, we first have to analyze the forces a beating cilium exerts on the surrounding fluid. Lengths and beating frequencies of cilia are very different for different organisms. Here, we focus on monocilia performing a rotational motion.[40] Because their length $L \simeq 2-3$ μm (Ref. 41) is much larger than their thickness [radius $a \simeq 0.1$ μm (Ref. 42)], one can describe the motion of the cilium as being created by a set of forces localized at the centerline of the cilium. The beating frequencies are of the order $f=\omega/2\pi \simeq 10$ s^{-1}.[12,41] The ciliary beating is thus characterized by a low Reynolds number, Re$\simeq 10^{-4}$, and the motion of the cilium is completely overdamped. For sufficiently small systems (typical extensions of a few 100 μm), momentum injection is instantaneous and the velocity field in the surrounding fluid induced by the beating cilium is a solution of the Stokes equation,

$$\eta \nabla^2 \boldsymbol{v} = \nabla p + \boldsymbol{F}\,\delta(\boldsymbol{r}-\boldsymbol{r}_t). \tag{1}$$

Here, $\boldsymbol{v}=\boldsymbol{v}(\boldsymbol{r})$ is the velocity in the fluid at position $\boldsymbol{r}$, $p=p(\boldsymbol{r})$ is the distribution of pressure, η is the viscosity of the surrounding fluid (i.e., water), and $\boldsymbol{F}$ is the force acting on the cilium moving on the trajectory $\boldsymbol{r}_t$.

In our approach, the forces driving the ciliary motion are prescribed and not calculated from the bending deformations of the ciliary filament as in, e.g., Refs. 28 and 43. In the case of a single monocilium, these forces result in an essentially circular trajectory. To obtain the velocity fields, we follow the "discrete cilia model" and reduce the rotating monocilium to a spherical bead of radius a that follows a closed trajectory at a height h above the lipid membrane; see Fig. 1. In Ref. 24, this trajectory was enforced to be exactly circular by a holonomic constraint. We relax this constraint here and allow for some radial flexibility by introducing a radial re-

storing force. The position of the bead is then best described by polar coordinates, the radius R, and the phase angle φ.

The restoring force $\boldsymbol{F}_r$ is assumed to be harmonic, $\boldsymbol{F}_r \cdot \boldsymbol{e}_R = F_r = -\lambda(R-R_0)$, where $\boldsymbol{e}_R$ denotes the unit vector in radial direction. The equilibrium radius R_0 is in the range of the length of the cilium.[40] The "spring constant" λ is determined by the bending rigidity κ and length L of the cilium: $\lambda = \kappa/L^3$. In Ref. 43, the bending rigidity was estimated for monocilia, based on their structure, $\kappa \simeq 4 \times 10^{-22}$ N m^2. This results in a large $\lambda \simeq 10^{-5}-10^{-4}$ N/m, which assures that the radius of the trajectory will deviate only slightly from the equilibrium value R_0, as shown below.

The effect of the dynein motors[44] is represented by an internal driving force $\boldsymbol{F}_{\text{in}}$ on the bead. We presume that this force has a constant absolute value and only acts in angular direction, $\boldsymbol{F}_{\text{in}} \cdot \boldsymbol{e}_\varphi = F_{\text{in}} = \text{const}$, where $\boldsymbol{e}_\varphi$ is the angular unit vector. The driving force F_{in} of course sets the beating frequency.

Because the motion of cilia is completely overdamped, the equation of motion of the bead is given by the balance of forces acting on it, namely drag, driving, and restoring force,

$$\boldsymbol{F}_d + \boldsymbol{F}_{\text{in}} + \boldsymbol{F}_r = \boldsymbol{0}. \tag{2}$$

The drag force exerted on spherical objects at very low Reynolds numbers is given by Stokes' law,

$$\boldsymbol{F}_d = -6\pi\eta a \boldsymbol{u} = -\zeta \boldsymbol{u}, \tag{3}$$

where $\boldsymbol{u}$ denotes the relative velocity of the bead with respect to the surrounding fluid, and $\zeta = 6\pi\eta a$ is the friction coefficient. In polar coordinates, the complete equations of motion then read

$$\zeta R \dot{\varphi} = F_{\text{in}}, \tag{4}$$

$$\zeta \dot{R} = -\lambda(R - R_0). \tag{5}$$

Because $a \simeq 0.1$ μm, one has $\zeta \simeq 2 \times 10^{-9}$ N s/m and $\lambda/\zeta \simeq (5 \times 10^3) - (5 \times 10^4)$ s^{-1}. Hence, the radial dynamics is much faster than the angular one (determined by $\omega \simeq 2\pi \times 10$ s^{-1}) and one can indeed conclude that the single cilium moves with a constant phase velocity ω on a circular trajectory,

$$\dot{\varphi} = F_{\text{in}}/(\zeta R_0) = \omega, \tag{6}$$

$$R = R_0. \tag{7}$$

Then, the relation between driving force and rotation frequency is simply $F_{\text{in}} = \zeta R_0 \omega$. We show now that this simple representation of a cilium is complex enough to lead to synchronization of motion with its neighbors.

III. HYDRODYNAMIC INTERACTIONS BETWEEN TWO CILIA

Typically, cilia belong to an array and are thus influenced by the fluid motion produced by their neighbors. To illustrate the effects on their motion, we consider two neighboring cilia with intrinsic frequencies ω_1 and ω_2. The noninteracting cilia are described by Eqs. (4) and (5). The velocity field induced by cilium 2 modifies the equation of motion of cilium 1 according to[45,46]

$$\zeta(R_1 \dot{\varphi}_1 - \boldsymbol{e}_{\varphi_1} \cdot \boldsymbol{v}_{12}) = F_{\text{in}} = \zeta R_0 \omega_1, \tag{8}$$

$$\zeta(\dot{R}_1 - \boldsymbol{e}_{R_1} \cdot \boldsymbol{v}_{12}) = -\lambda(R_1 - R_0). \tag{9}$$

Here, $\boldsymbol{v}_{12}$ denotes the fluid velocity field induced by cilium 2 at the position of cilium 1. Furthermore, $\boldsymbol{e}_{R_i}$ and $\boldsymbol{e}_{\varphi_i}$ are the unit vectors in the radial and angular directions, respectively, given in polar coordinates R_i and φ_i for cilium i by

$$\boldsymbol{e}_{R_i}(t) = (-\sin\varphi_i(t), \cos\varphi_i(t), 0), \tag{10}$$

$$\boldsymbol{e}_{\varphi_i}(t) = (-\cos\varphi_i(t), -\sin\varphi_i(t), 0). \tag{11}$$

Then, the position of cilium $i=1$ or 2 is given by (see Fig. 1)

$$\boldsymbol{r}_i(t) = ((i-1)l, 0, h) + R_i(t)\boldsymbol{e}_{R_i}(t) \tag{12}$$

$$= (-R_i(t)\sin\varphi_i(t) + (i-1)l, R_i(t)\cos\varphi_i(t), h), \tag{13}$$

where l is the distance between the centers of the two trajectories.

If the no-slip boundary condition at the wall is not taken into account, then $\boldsymbol{v}_{12}$ is given by[47]

$$\boldsymbol{v}_{12} = \frac{\boldsymbol{s} + \boldsymbol{n}_{12}(\boldsymbol{s} \cdot \boldsymbol{n}_{12})}{|\boldsymbol{r}_{12}|} + \mathcal{O}((a/r_{12})^3 \boldsymbol{s}), \tag{14}$$

where $\boldsymbol{s}$ is the strength of a Stokeslet, $\boldsymbol{n}_{12} \equiv \boldsymbol{r}_{12}/|\boldsymbol{r}_{12}|$, and $\boldsymbol{r}_{12}$ is the vector pointing from bead 2 to 1. The strength of the Stokeslet is given by the velocity of cilium 2,

$$\boldsymbol{s} = \frac{3a}{4}\dot{\boldsymbol{r}}_2 = \frac{3a}{4} R_2 \dot{\varphi}_2 \boldsymbol{e}_{\varphi_2} + \frac{3a}{4}\dot{R}_2 \boldsymbol{e}_{R_2}$$

$$= \frac{3a}{4} R_2 \dot{\varphi}_2 \boldsymbol{e}_{\varphi_2} + \mathcal{O}(R_0 \omega_1 a^2/l), \tag{15}$$

where we have used that the velocity field of cilium 1 induces a maximal radial disturbance $R_2 - R_0 \simeq (3/2) R_1 \omega_1 (\zeta/\lambda) a/l$. Then, Eq. (9) implies that R_2 decays faster than the solution of $\dot{R}_2 \simeq 2(\lambda/\zeta)(R_2 - R_0) \simeq 3 R_0 \omega_1 a/l$.

If the no-slip boundary condition on the wall is taken into account, the velocity field becomes[28]

$$\boldsymbol{v}_{12} = 12 h^2 \frac{\boldsymbol{n}_{12}(\boldsymbol{s} \cdot \boldsymbol{n}_{12})}{|\boldsymbol{r}_{12}|^3} + \mathcal{O}(a^3 h^2 \boldsymbol{s}/r_{12}^5). \tag{16}$$

Note that in the derivation of the last equation, $h/r_{12} \ll 1$ has been used, and therefore Eq. (16) does not reduce to Eq. (14) as h approaches ∞.

As shown in Appendix A, the equations of motion (8)–(16) can be explicitly solved for $\dot{\varphi}_i$ and R_i in the limit $R \ll l$, yielding

$$\dot{\varphi}_1 = (R_0/R_1)\omega_1 - (R_2/R_1)\rho J(\varphi_1, \varphi_2)\dot{\varphi}_2, \tag{17}$$

$$R_1 = R_0 + \alpha \rho R_2 K(\varphi_1, \varphi_2)\dot{\varphi}_2, \tag{18}$$

$$\dot{\varphi}_2 = (R_0/R_2)\omega_2 - (R_1/R_2)\rho J(\varphi_2, \varphi_1)\dot{\varphi}_1, \tag{19}$$

$$R_2 = R_0 + \alpha\rho R_1 K(\varphi_2,\varphi_1)\dot{\varphi}_1, \tag{20}$$

where we have rescaled time by $\bar{\omega}$, and ω_1 and ω_2 are measured in units of $\bar{\omega}$. Here, $\bar{\omega}$ represent a typical frequency, e.g., $\bar{\omega}\equiv\max\{\omega_1,\omega_2\}$ or $\bar{\omega}\equiv\sqrt{\omega_1\omega_2}$. Furthermore, the interactions are given in leading order by

$$J(\varphi_i,\varphi_j) \equiv -\mu\cos(\varphi_i-\varphi_j) - \cos(\varphi_i+\varphi_j), \tag{21}$$

$$K(\varphi_i,\varphi_j) \equiv \mu\sin(\varphi_i-\varphi_j) + \sin(\varphi_i+\varphi_j). \tag{22}$$

The equations of motion also depend on the "ciliary density" ρ (i.e., the number of cilia per unit of length), and on the time scale of the radial motion α given by

$$\rho \equiv \frac{1}{2l}\frac{3a}{4}(\sqrt{12}h/l)^{\nu}, \tag{23}$$

$$\alpha \equiv \bar{\omega}\zeta/\lambda. \tag{24}$$

The two parameters μ and ν are introduced so that the cases with and without a wall can be treated in parallel. In particular, the functional forms for the interactions (21) and (22) are the same, only their strengths change, as determined by $(\mu,\nu)=(3,0)$ and $(\mu,\nu)=(1,2)$ for the case without and with no-slip boundary conditions on the membrane, respectively.

The equation of motion for cilium 2 can be directly obtained from that for cilium 1 by interchanging indices 1 and 2. This is a direct consequence of our assumption that the cilia are far from each other, $R \ll l$, and thus $\boldsymbol{n}_{12} = -\boldsymbol{e}_x + \mathcal{O}(R/l)$; see Appendix A.

Because terms of order R/l have already been neglected in the interaction terms, the equations of motion are given in leading order by

$$\dot{\varphi}_1 = \omega_1 - \rho\omega_2 J(\varphi_1,\varphi_2) - \rho\alpha\omega_1\omega_2 K(\varphi_1,\varphi_2), \tag{25}$$

$$\dot{\varphi}_2 = \omega_2 - \rho\omega_1 J(\varphi_2,\varphi_1) - \rho\alpha\omega_1\omega_2 K(\varphi_2,\varphi_1). \tag{26}$$

For constant radii $R_i = R_0$ corresponding to $\alpha=0$, the equations of motion reduce to those of Ref. 24. As shown there, in this case neither synchronization nor phase locking occurs. However, as we show now, the flexibility in the radial motion introduced here (corresponding to $\alpha\neq 0$) is sufficient to lead to synchronized motion of two cilia.

IV. PHASE LOCKING AND SYNCHRONIZATION OF TWO CILIA

In this section, we analyze the conditions under which the motion of the two cilia becomes synchronized ($\varphi_1=\varphi_2$) or phase locked ($\dot{\varphi}_1=\dot{\varphi}_2$). To do so, it is useful to consider the phase difference $\chi\equiv\varphi_1-\varphi_2$ between the two neighboring cilia. According to Eqs. (25) and (26), it obeys

$$\dot{\chi} = (\omega_1-\omega_2)(1+\rho J(\varphi_1,\varphi_2)) - \gamma\sin\chi, \tag{27}$$

where $\gamma\equiv 2\mu\alpha\rho\omega_1\omega_2 > 0$. As will become clear during the following analysis, γ sets the time scale for synchronization. To analyze Eq. (27), it is useful to distinguish between the cases $\omega_1=\omega_2$ and $\omega_1\neq\omega_2$.

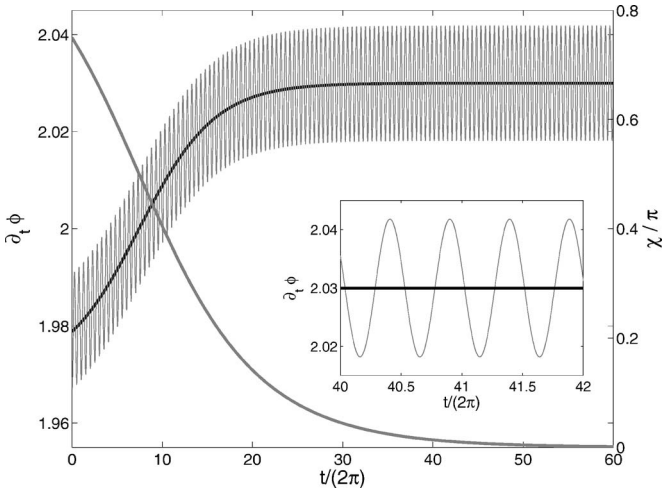

FIG. 2. Time dependence of $\chi=\varphi_1-\varphi_2$ and $\dot{\phi}=\dot{\varphi}_1+\dot{\varphi}_2$ for a pair of cilia. Data are for $\omega_1=\omega_2$, $\mu=3$, $\rho=0.005$, $\alpha=0.1\bar{\omega}$, and initial conditions $\chi_0=\phi_0=\frac{3}{4}\pi$. Shown are (i) the phase difference $\chi(t)/\pi$ obtained from Eq. (28) (gray bold line), (ii) the mean total velocity $\langle\dot{\phi}\rangle(t)$, given by Eq. (30) (black bold line), and (iii) total velocity $\dot{\phi}(t)$ (thin gray line) obtained by numerically integrating Eq. (29). In the synchronized state, the total velocity oscillates with a frequency $\Omega\equiv 2\omega+2\beta$ (shown in the inset); see Eq. (29) and Fig. 3.

A. Same intrinsic frequency: $\omega_1=\omega_2$

We first consider the case in which both cilia beat with the same intrinsic frequency $\omega_1=\omega_2$. In this case, Eq. (27) has two fixed points, an unstable one at $\chi_u=\pi$ and a stable one at $\chi_s=0$.

This can also be seen from the explicit solution

$$\chi(t) = 2\arctan(\tan(\chi_0/2)\cdot e^{-\gamma t}), \tag{28}$$

showing that for any initial condition eventually $\chi_s=0$ is reached. Thus, the two cilia synchronize on a time scale that is inversely proportional to γ.

As the cilia synchronize, their angular velocity increases. This is a direct consequence of our assumption that the driving force is constant, since friction is minimal for vanishing phase difference. To see this more formally, consider the sum of phases $\phi=\varphi_1+\varphi_2$ and its equation of motion

$$\dot{\phi} = 2\omega + 2\omega\rho(\mu\cos\chi + \cos\phi) - (\gamma/\mu)\sin\phi. \tag{29}$$

At this point, it is convenient to neglect small velocity variations by averaging over a revolution of the phases implying

$$\langle\dot{\phi}\rangle(t) = 2\omega + 2\beta\cos\chi(t), \tag{30}$$

where $\beta\equiv\mu\omega\rho$. This shows that as $\chi(t)$ decreases monotonically from χ_0 to zero, the mean velocity increases toward $2\omega+2\beta$; see Fig. 2. Thus, β measures the increase in velocity. It should be noted that during synchronization, cilia with a phase difference $\chi(t)>\pi/2$ slow each other down, while for $\chi(t)<\pi/2$ the beating velocity increases. This can be made clear geometrically; see Fig. 3.

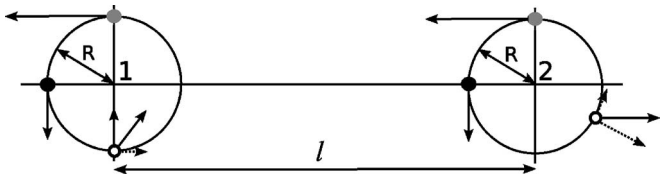

FIG. 3. Synchronization mechanism for two cilia with identical intrinsic frequencies ω and large interciliary distance $R \ll l$. (i) Nonsynchronized cilia (hollow circles): Cilium 2 exerts a force on cilium 1 (shown as solid arrow) given by $\mathbf{F_{12}} = \zeta \mathbf{v_{12}} \propto \boldsymbol{s} + \boldsymbol{n}_{12}(\boldsymbol{s}\cdot\boldsymbol{n}_{12}) \propto \boldsymbol{e}_{\varphi_2} - \cos\varphi_2 \boldsymbol{e}_x$; see Eq. (14). The dashed arrows shows the angular and radial component of this force. For trajectories with fixed radii, only the tangential contribution influences the dynamics leading only to a symmetric change in the speed of the two cilia (but no change of their relative phase). However, if the radius is allowed to vary, then in the depicted situation R_1 decreases, and R_2 increases leading to an increase in angular velocity of cilium 1, and a decrease in angular velocity of cilium 2. (ii) Synchronized cilia (filled circles): Both cilia have the same velocity, which oscillates around its mean value with a frequency Ω. The origin of this oscillation is that the drag between two beads moving behind each other (gray circles) is twice as large as for parallel motion (black circles).

B. Different intrinsic frequencies: $\omega_1 \neq \omega_2$

As a next step, we consider two cilia that are driven by (slightly) different internal forces giving rise to (slightly) different intrinsic frequencies $\omega_1 \neq \omega_2$. Equation (27) then becomes (in first order of the small quantities ρ and $\Delta\omega \equiv \omega_1 - \omega_2$)

$$\dot{\chi} = \Delta\omega - \gamma \sin\chi. \tag{31}$$

Thus, stationary solutions exist only for

$$|\Delta\omega| \leqslant \gamma, \tag{32}$$

and a minimal synchronization strength $\gamma_c = |\Delta\omega|$ is required for phase locking of ciliary motion. Here, the stable fixed point is given by

$$\chi_s = \arcsin\frac{\Delta\omega}{\gamma}. \tag{33}$$

Thus, for $\omega_1 \neq \omega_2$ the system becomes phase locked, but not synchronized, and the phases evolve with a constant, but nonvanishing phase shift, $\varphi_1(t) = \varphi_2(t) + \chi_s$. The time needed for phase locking increases with decreasing γ and diverges at the critical point γ_c.

As ω_1 approaches ω_2, one has $\gamma_c \to 0$, implying that even very weak interactions can already lead to synchronization. However, then the time scale on which synchronization occurs will become large.

As can be seen from the equations of motion [Eq. (27) or Eq. (31)], γ couples to the term $\sin\chi$, which is, due to its asymmetry, typically responsible for the synchronization and phase locking of coupled phase oscillators.[11] One should note that because $\gamma \propto \rho\alpha$, and α comes from the radial dynamics, it is crucial that the trajectories are allowed to have a variable radius.

The term $\cos\chi$ in Eq. (29) is responsible for the speed of the two cilia for both the synchronized and the nonsynchronized state. It is independent of α and thus also occurs for rigid trajectories.

At this point, it is worth noting that the results of our simple monocilia model agree very well with the numerical investigations of a more complicated model of rotating helices, introduced in Ref. 30. Details are given in Appendix B. Here, we want to emphasize that synchronization of rotating helices only occurs if the attachment of the helix to the cell wall is flexible.[30] This is similar to our finding that synchronization only occurs for finite α (in fact α^{-1} corresponds to the trap strength introduced in Ref. 30; see Appendix B for details). In this light, our model should be seen as a *minimal model* having all the relevant mechanisms responsible for synchronization of ciliary beating and (as shown below) metachronal wave formation.

V. CHAIN OF CILIA

As a next step, we consider a one-dimensional array of N cilia. If the no-slip boundary condition of the wall is taken into account, the hydrodynamic interactions between the beating cilia decay as l^{-3} with interciliary distance l; see Eq. (23). Here, we focus on $l \gg R$. Then, in good approximation only nearest neighbors interact in the array.

Furthermore, in this limit the equations of motion become particularly simple: The flow field felt by cilium i at position φ_i induced by a moving cilium j at position φ_j does not depend on whether cilium j is to the right or to the left of cilium i. Consequently, the equations of motion read

$$\dot{\varphi}_i = \omega_i - \rho \sum_{j\in\langle i\rangle} \omega_j J(\varphi_i, \varphi_j) - \rho\alpha\omega_i \sum_{j\in\langle i\rangle} \omega_j K(\varphi_i, \varphi_j), \tag{34}$$

where $\langle i\rangle$ denotes the nearest neighbors of cilium i. The cilia have intrinsic frequencies ω_i (again measured in units of an appropriately chosen $\bar{\omega}$). For nonperiodic boundary conditions, the first and last cilium in the chain have only one neighbor to interact with.

As discussed in the last section, the terms $\cos(\varphi_i + \varphi_j)$ and $\sin(\varphi_i + \varphi_j)$ in Eqs. (34), (21), and (22) only describe fluctuations around the mean velocity and thus are only important for the short-term behavior of the system. Upon averaging over one period these terms drop out, and we obtain the effective equation of motion,

$$\dot{\varphi}_i = \omega_i + \mu\rho \sum_{j\in\langle i\rangle} \omega_j \cos(\varphi_i - \varphi_j) - \mu\rho\alpha\omega_i \sum_{j\in\langle i\rangle} \omega_j \sin(\varphi_i - \varphi_j). \tag{35}$$

However, the omitted terms prevent the system from becoming properly phase locked: A state with $\dot{\varphi}_i = \dot{\varphi}_j$ for $i,j = 1,\ldots,N$ cannot be reached since the velocity variations are also phase-shifted. Instead, only the *mean velocities* $\tilde{\omega}_i = \lim_{t\to\infty}[\varphi_i(t) - \varphi_i(0)]/t$ will adapt, resulting in an *entrained state* $\tilde{\omega}_i = \tilde{\omega}_j$.

A. Identical intrinsic frequencies and periodic boundary conditions

First, we consider the case of identical intrinsic frequencies $\omega_i = \omega$ and periodic boundary conditions (where the first and the last cilium in the chain are neighbors resulting in a ringlike chain). In this case, as we show now, phase-locked

states with a constant phase difference between neighboring cilia are stable if the phase difference is below a critical threshold. These stable states correspond to traveling waves with a constant wavelength and are called *metachronal waves* in the biological literature.[12] Upon introducing the phase differences

$$\chi_i \equiv \varphi_{i+1} - \varphi_i, \tag{36}$$

where $i=1,\ldots,N \pmod N$, and the global phase

$$\Phi \equiv \frac{1}{N}\sum_{j=1}^{N} \varphi_j, \tag{37}$$

Eq. (35) separates into equations for the χ_i,

$$\dot{\chi}_i = \beta(\cos\chi_{i+1} - \cos\chi_{i-1}) + \frac{\gamma}{2}(\sin\chi_{i+1} - 2\sin\chi_i + \sin\chi_{i-1}), \tag{38}$$

and one equation for the mean velocity,

$$\dot{\Phi} = \omega + \frac{2\beta}{N}\sum_{j=1}^{N} \cos\chi_j. \tag{39}$$

Again, $\beta=\mu\rho\omega$ and $\gamma=2\mu\alpha\rho\omega^2$. Out of the N variables entering Eq. (38), only $N-1$ are independent, since the phase difference between the first and the last cilium is given by

$$\chi_N = -\sum_{j=1}^{N-1} \chi_j. \tag{40}$$

Metachronal waves with a constant phase difference $\chi_i=\psi$ are stationary solutions of Eq. (38) if $\psi\cdot N=2\pi\cdot M$, where the integer $M=0,\ldots,N-1$. Not all of these waves are stable: In order to determine their stability, we transform to a coordinate system comoving with the cilia. The mean velocity is given by

$$\dot{\Phi} = \omega + 2\beta\cos\psi \equiv \tilde{\Omega}. \tag{41}$$

As for a pair of cilia, in the case of $|\psi|<\pi/2$ this phase speed is higher than for noninteracting cilia; the increase is twice as high as for a pair of cilia [see Eq. (29)] because each cilium interacts with two neighbors. The equations of motion for the relative phase $\xi_i\equiv\varphi_i-\tilde{\Omega}t$ then become

$$\dot{\xi}_i = \beta[\cos(\xi_{i+1}-\xi_i) + \cos(\xi_i-\xi_{i-1}) - 2\cos\psi] + \frac{\gamma}{2}[\sin(\xi_{i+1}-\xi_i) - \sin(\xi_i-\xi_{i-1})]. \tag{42}$$

The metachronal wave then has $\xi_{j+1}=\xi_j+\psi$, and is a fixed point of Eq. (42). Its stability is determined by the eigenvalues of the linearization of this equation. The resulting matrix belongs to the class of circulant matrices, where the spectrum can be calculated explicitly (see Ref. 48 and Appendix C). One finds that the eigenvalues are given by

$$\max_m \mathrm{Re}(\lambda_m) = \begin{cases} 0 & \text{for } |\psi| \leqslant \pi/2 \\ -2\gamma\cos\psi > 0 & \text{for } |\psi| > \pi/2 \end{cases}. \tag{43}$$

Thus, waves with $|\psi|\leqslant\pi/2$ (including the synchronized state $\psi=0$) are in linear order only marginally stable, while all waves with phase differences $|\psi|>\pi/2$ are unstable. The eigenvector to the marginally stable eigenvalue 0 is constant in all the ξ_i and hence reflects the invariance under a shift of the total phase. Note that the stability properties hold for all $\rho>0$ and $\alpha>0$.

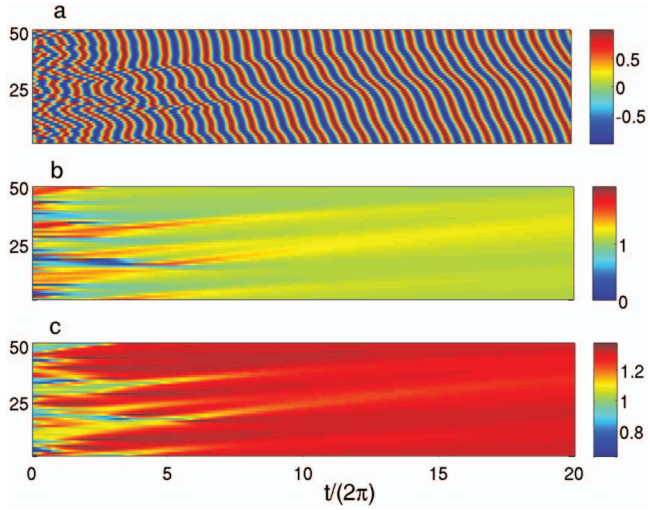

FIG. 4. (Color) Early stages of the formation of a metachronal wave for 50 identical cilia with periodic boundary conditions, as observed numerically starting from a random distribution of initial phases $\varphi_{i,0}$. (a) Color code plot of $\sin\varphi_i(t)$ as a function of time (where i is drawn on the y axis). (b) Phase differences $\chi_i(t)$ between neighboring cilia as a function of time. We have chosen to color code $(\chi_i(t)-\pi)/\pi$ [where $\chi_i(t)-\pi$ is taken mod 2π]. (c) $\dot{\varphi}_i(t)$ as a function of time. As one can see by direct inspection, the metachronal wave forms by merging of different regions where cilia have spontaneously built up a constant phase difference. The metachronal wave formation occurs simultaneously with the increase in $\dot{\varphi}_i$. The time required to form the metachronal wave depends on γ. Ultimately, all phase differences $\chi_i=2\pi(3/50)$ (see Fig. 5) corresponding to a wavelength $Nl/3$. Data are for parameter values $\mu=3$, $\rho=0.0524$, $\alpha=0.01\bar{\omega}$.

In numerical simulations, the formation of metachronal waves (see Figs. 4 and 5) is observed if α exceeds a critical threshold, i.e., if the cilia are assumed to be flexible enough. The decay of a metachronal wave with $|\psi|>\pi/2$ is shown in Fig. 6.

B. Identical intrinsic frequencies and free boundaries

We now analyze chains with free boundaries. Again, the cilia are assumed to have identical intrinsic frequencies $\omega_i=\omega$. If cilium 1 has the leftmost and cilium N the rightmost position in the chain, then the equations for the phase differences (38) are unchanged for $i=2,\ldots,N-2$. The phase differences involving the cilia at the ends are given by

$$\dot{\chi}_1 = \beta\cos\chi_2 + \frac{\gamma}{2}(\sin\chi_2 - 2\sin\chi_1), \tag{44}$$

$$\dot{\chi}_{N-1} = -\beta\cos\chi_{N-2} + \frac{\gamma}{2}(-2\sin\chi_{N-1} + \sin\chi_{N-2}). \tag{45}$$

Evidently, a metachronal wave with a constant phase shift $\chi_i=\psi$ is not a solution of these equations. However, in this geometry a different kind of wave is observed when the cilia are sufficiently flexible, i.e., α is large enough. Figure 7 shows a numerical example. Here, the wave emanates from

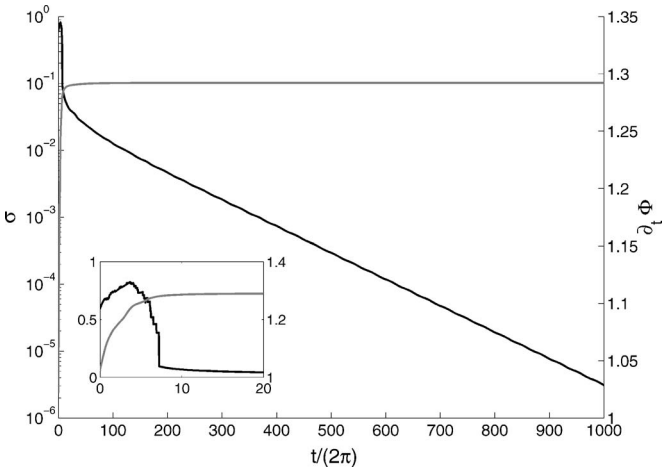

FIG. 5. Long-time behavior of the standard deviation of the phase differences $\sigma(\chi_i(t))=\sqrt{(1/N)\Sigma_i(\chi_i(t)-\bar{\chi}(t))^2}$ (black line) and the mean of the phase velocities $\dot{\Phi}(t)$ (gray line) calculated from the same numerical data as in Fig. 4. The inset, showing the first 20 periods, demonstrates that even though most of the rearrangements to locally form metachronal waves occur within the first few periods (see Fig. 4), the standard deviation $\sigma(t)$ is still large, due to the different wave numbers of these waves. Eventually, the state given by $\varphi_n=\varphi_0+n\psi$, where $\psi=(3/25)\pi$, is approached exponentially (indicating its stability). The resulting mean velocity can be calculated from Eq. (41) and also yields an increase of 29%, in agreement with the numerical data shown in the inset.

the center and spreads toward the ends. The phase differences are nearly constant on each side of the chain, but reflection symmetric with respect to the center, i.e., one has

$$\chi_i \simeq \psi, \quad \text{for } i=1,\ldots,N/2-1, \tag{46}$$

$$\chi_{N/2} \simeq 0, \tag{47}$$

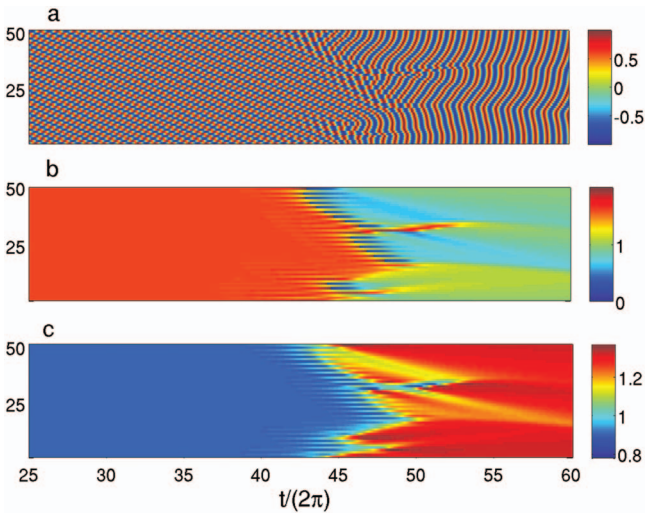

FIG. 6. (Color) Unstable metachronal wave. As in Fig. 4, we show (a) $\sin\varphi_i(t)$, (b) $[(\chi_i(t)-\pi)\bmod 2\pi]/\pi$, and (c) $\dot{\varphi}_i(t)$. The parameters are the same as in Fig. 4, but the initial condition is chosen to be a metachronal wave with constant phase difference $\psi=(3/5)\pi$. This wave is unstable and eventually evolves toward a metachronal wave with $\psi=-(4/50)\pi$. Note that the phase velocities $\dot{\varphi}_i$ are initially identical, but smaller than the intrinsic frequencies ω_i, since the neighboring cilia slow each other down if $|\psi|>\pi/2$.

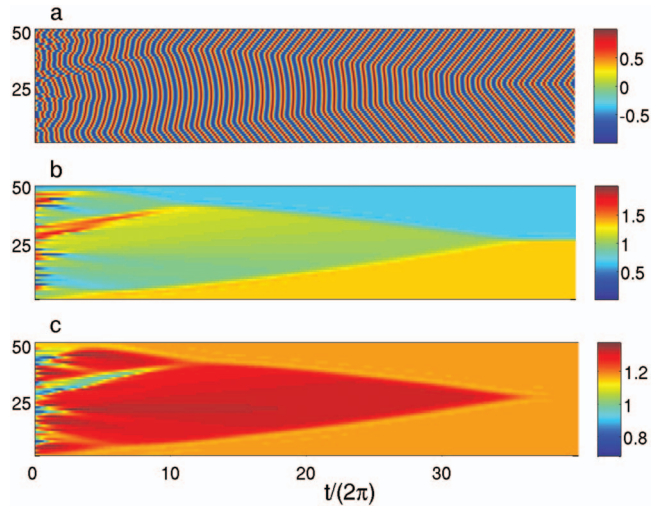

FIG. 7. (Color) Collective beating in a ciliary chain with free ends. In this geometry, metachronal waves are not stable. However, the cilia beat in a wavelike fashion. The cilia left of the center have nearly identical phase shift and the cilia right of the center also have nearly the same phase shift but with opposite sign. Formation of the collective beating emanates from the boundaries. Once, the cilia beat cooperatively, the wave moves from the middle to the boundaries. [Data shown are for the same set of parameters as in Figs. 4 and 6, again (a) $\sin\varphi_i(t)$, (b) $(\chi_i(t)/\pi-1)\bmod 2$, and (c) $\dot{\varphi}_i(t)$.]

$$\chi_i \simeq -\psi, \quad \text{for } i=N/2+1,\ldots,N/2 \tag{48}$$

(where for simplicity it has been assumed that N is even).

These waves are not the only steady-state solutions of the phase difference equation. For smaller α, we numerically find also waves that travel from one side of the chain to the other; see Fig. 8. They are not exactly metachronal, but have small oscillations in the wavelength.

Again, the investigation of an oscillator chain with nearest-neighbor interactions and uniform frequency distribution is motivated by biological systems. In the context of synchronization, such systems have only rarely been studied. Reference 49 is an example. But there it is assumed that the interaction vanishes in the synchronized state. For our interactions [given by Eqs. (21) and (22)] this is not the case.

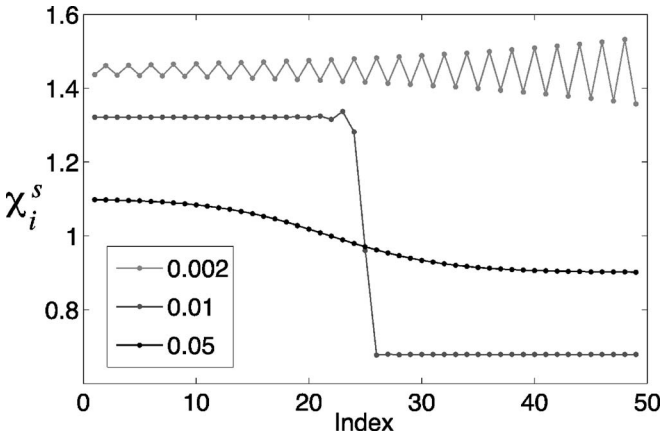

FIG. 8. Steady-state values of the phase differences χ_i^s for the ciliary chain with free ends. All parameters with the exception of α are taken from the previous numerical runs. Shown are $(\chi_i^s-\pi)/\pi$ (where $\chi_i^s-\pi$ is taken mod 2π) for (i) $\alpha=0.002\bar{\omega}$ (light gray), (ii) $\alpha=0.01\bar{\omega}$ (dark gray), and (iii) $\alpha=0.05\bar{\omega}$ (black).

We conclude this section by showing results from a numerical simulation for a chain where the frequencies of the individual cilia are not identical. If the relative variations between frequencies are small, $|\omega_i-\omega_j| \ll \bar{\omega}$, the product of the small quantities ρ and $\Delta\omega_j=\omega_j-\bar{\omega}$ can be neglected and in leading order Eq. (35) reduces to

$$\dot{\varphi}_i = \omega_i + \mu\rho\bar{\omega} \sum_{j\in\langle i\rangle} [\cos(\varphi_i - \varphi_j) - \alpha\bar{\omega} \sin(\varphi_i - \varphi_j)]. \quad (49)$$

Preliminary numerical calculations indicate that this model indeed can lead to phase locking provided that the variations in the intrinsic frequencies are sufficiently small, the cilia are not too rigid, and the hydrodynamical interactions are strong enough. The (unphysical) case where the antisymmetric part of the coupling dominates, i.e., $\alpha \gg 1$, can be studied analytically.

These results are in agreement with observations on models with localized interactions and various frequencies, such as the ones studied in Refs. 38 and 39. However, as for Ref. 49, the results of Ref. 38 do not cover our case since the coupling function lacks the required symmetry. In this sense, our model is closer to the ones studied by Sakaguchi *et al.*,[39] where various general entrained states but no metachronal waves are discussed.

VI. CONCLUSION AND OUTLOOK

We have developed a model for hydrodynamically interacting monocilia that is both simple enough to be analytically tractable but complex enough to describe the synchronization properties of the cilia. It thus bridges the gap between idealized but well understood models for phase synchronization (such as those studied in Refs. 11 and 31–39), and realistic ones, which are derived from first principles, but are too complicated to be understood analytically (see, e.g., Refs. 27–29 and 50). In our model, the (circular) trajectory of a cilium is not exactly prescribed since we allow some flexibility in the radius. It turns out that this additional degree of freedom breaks the symmetry in the interactions and introduces the coupling that leads to synchronization and cooperative ciliary motion.

The synchronization process is particularly simple to analyze in a system with two interacting cilia. Their motion always phase-locks, provided that the ciliary density ρ exceeds a critical threshold set by the difference of the intrinsic frequencies. For cilia with identical intrinsic frequencies, the synchronized state is always reached. In both cases, the cilia speed up as their phase difference decreases and the hydrodynamical drag is reduced. These results are very similar to those obtained numerically for a much more complicated model for hydrodynamically interacting helices.[30] This supports our claim that we have developed a minimal model for the theoretical description of the synchronization properties of rotating entities that interact via a Stokes fluid.

In a next step, we have considered chains of cilia. For periodic boundary conditions and identical intrinsic frequencies, metachronal waves are stable if their wavelength exceeds a critical threshold given by four times the interciliary distance. This agrees well with the experimentally observed wavelength of metachronal waves.[19] The waves also form spontaneously, if the filaments are not too rigid. For free ends, metachronal waves are not even a solution of the equations of motion for the coupled beating. But different phase-locked states form, again, provided that the filaments are not too rigid. For sufficiently high flexibility, these states represent waves traveling from the middle to the edges of the array. We also have shown analytically that this collective motion goes hand in hand with an increase in ciliary speed, increasing the efficiency of the associated fluid transport or locomotion. This effect is due to the symmetric part in the coupling function, whereas synchronization and metachronal wave formation are based on the (weaker) asymmetric part.

The monocilia model developed seems to have all ingredients required to describe collective effects in ciliary chains and it should provide a good basis for the development of models for more complicated beating patterns. For this purpose, it will be necessary to analyze in detail the bending deformations a cilium undergoes. In particular, the single phase approximation developed in Ref. 24 will have to be generalized to motions with variable amplitudes. With such a description, it should be possible to analytically describe the beating of many cilia, and not only (rotating) monocilia.

ACKNOWLEDGMENTS

This work was partly supported by the Deutsche Forschungsgemeinschaft and by the Fonds der Chemischen Industrie.

APPENDIX A: CALCULATION OF THE EQUATIONS OF MOTION FOR TWO CILIA

Here, we derive Eqs. (17) and (18) for $\dot{\varphi}_1$ and R_1 of cilium 1. In doing so, we assume $R \ll l$ (thus also $a \ll l$) and neglect terms of order aR/l^2.

By inserting Eqs. (11)–(15) into Eq. (8), one has (with $\boldsymbol{e}_x$ denoting the unit vector pointing in the x direction)

$$\boldsymbol{e}_{\varphi_1} \cdot \boldsymbol{s} = \frac{3a}{4} R_2 \dot{\varphi}_2 \cos(\varphi_1 - \varphi_2), \quad (A1)$$

$$\boldsymbol{r}_{12} \equiv \boldsymbol{r}_1 - \boldsymbol{r}_2 = -l\boldsymbol{e}_x + \mathcal{O}(R), \quad (A2)$$

$$|\boldsymbol{r}_{12}|^{-1} = l^{-1}(1 + \mathcal{O}(R/l)), \quad (A3)$$

$$\boldsymbol{n}_{12} = -\boldsymbol{e}_x + \mathcal{O}(R/l), \quad (A4)$$

$$\boldsymbol{e}_{\varphi_1} \cdot \boldsymbol{n}_{12} = \cos\varphi_1 + \mathcal{O}(R/l), \quad (A5)$$

$$\boldsymbol{s} \cdot \boldsymbol{n}_{12} = \frac{3a}{4} R_2 \dot{\varphi}_2 (\cos\varphi_2 + \mathcal{O}(R/l)), \quad (A6)$$

implying

$$\boldsymbol{e}_{\varphi_1} \cdot \boldsymbol{v}_{12} = \frac{3a}{8l} R_2 \dot{\varphi}_2 \times (3\cos(\varphi_1 - \varphi_2) + \cos(\varphi_1 + \varphi_2) + \mathcal{O}(R/l)), \quad (A7)$$

which finally leads to Eq. (17). Equation (18) follows from

$$\boldsymbol{e}_{R_1} \cdot \boldsymbol{s} = \frac{3a}{4} R_2 \dot{\varphi}_2 \sin(\varphi_1 - \varphi_2), \tag{A8}$$

$$\boldsymbol{e}_{R_1} \cdot \boldsymbol{n}_{12} = \sin \varphi_1 + \mathcal{O}(R/l), \tag{A9}$$

yielding

$$\boldsymbol{e}_{R_1} \cdot \boldsymbol{v}_{12} = \frac{3a}{8l} R_2 \dot{\varphi}_2 \times [3 \sin(\varphi_1 - \varphi_2) + \sin(\varphi_1 + \varphi_2) + \mathcal{O}(R/l)]. \tag{A10}$$

The results for the case with the no-slip wall can be derived in a similar way.

APPENDIX B: COMPARISON WITH NUMERICAL RESULTS FOR ROTATING HELICES

Here, we compare the results of our simple model for two interacting cilia with the numerical findings for two rotating helices derived in Ref. 30. There, a single helix is modeled as a collection of rigidly connected beads forming a helical shape. The two helices are driven by a constant torque and interact via the surrounding (Stokes) fluid. Their position in space is fixed with their end points anchored in harmonic traps. This system was studied numerically by using the method of mobility tensors.

To directly compare our results with those of Ref. 30, we rescale time by $\tau \equiv (t - t_{\pi/2}) \gamma \cdot 2/\pi$, where $t_{\pi/2}$ denotes the time at which $\chi = \pi/2$, given by $t_{\pi/2} = \gamma^{-1} \log(\tan(\chi_0/2))$. Note that initial phase differences smaller than $\pi/2$ have negative $t_{\pi/2}$. Upon rescaling Eq. (28), one finds

$$\chi(\tau) = 2 \arctan(e^{-\pi\tau/2}). \tag{B1}$$

This equation describes well the numerical data shown in Fig. 4 of Ref. 30.

Upon rescaling time, one finds

$$\langle \partial_t \phi \rangle(\tau) = 2\omega + 2\mu\omega\rho \cos \chi(\tau) = 2\omega + 2\mu\omega\rho \tanh\left(\frac{\pi}{2}\tau\right), \tag{B2}$$

which is also in agreement with the increase in speed found in Ref. 30.

Reichert and Stark also find that the synchronization speed $|d\chi/dt|$ scales as $\tanh(cK^{-1})$ as a function of the trap strength K and a fitting parameter c. For strong traps, this agrees with our model, where the synchronization speed is proportional to γ and thus to the parameter α quantifying the radial flexibility. Finally, the torques acting on the helices were assumed to be (slightly) different giving rise to a torque difference ΔD. This ΔD corresponds to our $\Delta\omega$. Precisely like in our treatment in Sec. IV B, phase-locking only occurs if the torque difference ΔD is below a critical threshold ΔD_c. As anticipated, the resulting phase lag is zero for vanishing torque difference and $\pi/2$ for the maximum torque difference. The phase lag as a function of $\Delta D/\Delta D_c$ (shown in Fig. 8 in Ref. 30) is well described by $\chi = \arcsin(\Delta D/\Delta D_c)$ (data not shown), as predicted by Eq. (33).

APPENDIX C: EIGENVALUE CALCULATION

In this appendix, we calculate the eigenvalues of the Jacobian for a chain of cilia and determine the eigenvalue with the largest real part. The Jacobian at $\xi_j = j\psi$ is given by

$$D_{i,j} \equiv \left.\frac{\partial \dot{\xi}_i}{\partial \xi_j}\right|_{\xi_j = j\psi} = \beta(\delta_{i-1,j} - \delta_{i+1,j}) \sin \psi + \frac{\gamma}{2}(\delta_{i-1,j} - 2\delta_{i,j} + \delta_{i+1,j}) \cos \psi. \tag{C1}$$

To this end, we utilize the fact that $(D_{i,j})$ is a "circulant" matrix, i.e., its successive rows are obtained by cyclic right-shifts of the first row.[48] An explicit formula for the eigenvalues is given in Ref. 48,

$$\lambda_m = D_{1,1} + D_{1,2}\theta^m + D_{2,1}\theta^{(N-1)m}, \tag{C2}$$

where $\theta = \exp(2\pi i/N)$ and m runs from 0 to $N-1$. Inserting the matrix elements yields

$$\lambda_m = -\gamma \cos \psi + \left(\frac{\gamma}{2} \cos \psi - \beta \sin \psi\right)\theta^m + \left(\frac{\gamma}{2} \cos \psi + \beta \sin \psi\right)\theta^{(N-1)m}. \tag{C3}$$

Because of the relations

$$\theta^{(N-1)m} + \theta^m = \theta^{-m} + \theta^m = 2 \cos(2\pi m/N), \tag{C4}$$

$$\theta^{(N-1)m} - \theta^m = \theta^{-m} - \theta^m = -2i \sin(2\pi m/N), \tag{C5}$$

the real parts of the eigenvalues are given by

$$\mathrm{Re}(\lambda_m) = \gamma \cos \psi(-1 + \cos(2\pi m/N)). \tag{C6}$$

Without loss of generality, $-\pi \leqslant \psi \leqslant \pi$. Now, for $|\psi| \leqslant \pi/2$ one has $\cos \psi \geqslant 0$ and λ_0 is the eigenvalue with the largest real part: $\mathrm{Re}(\lambda_0) = 0$. For $|\psi| > \pi/2$, all the eigenvalues have a positive real part except for λ_0. Furthermore, the largest value is reached when $\cos(2\pi m/N)$ is minimal, i.e., for $m = N/2$ (N even) and $m = (N-1)/2$ (N odd). Thus, one has $\max_m \mathrm{Re}(\lambda_m) = -2\gamma \cos \psi$ for N even and $\max_m \mathrm{Re}(\lambda_m) \simeq -2\gamma \cos \psi$ for N odd and large.

[1] A. Winfree, *The Geometry of Biological Time* (Springer, New York, 1980).
[2] S. Camazine, J.-L. Deneubourg, N. R. Franks, J. Sneyd, G. Theraulaz, and E. Bonabeau, *Self-Organization in Biological Systems* (Princeton University Press, Princeton, 2001).
[3] J. Buck and E. Buck, Science **159**, 1319 (1968).
[4] J.-M. Ramirez, A. K. Tryba, and F. Pea, Curr. Opin. Neurobiol. **14**, 665 (2004).
[5] R. Koenigsberger, M. abd Sauser, and J.-J. Meister, Bull. Math. Biol. **67**, 1253 (2005).
[6] R. Moore, Science **284**, 2102 (1999).
[7] S. H. Strogatz, D. M. Abrams, A. McRobie, B. Eckhardt, and E. Ott, Nature **438**, 43 (2005).
[8] B. Eckhardt, E. Ott, S. Strogatz, D. Abrams, and A. McRobie, Phys. Rev. E **75**, 021110 (2007).
[9] A. Pikovsky, M. Rosenblum, and J. Kurths, *Synchronization: A Universal Concept in Nonlinear Sciences* (Cambridge University Press, Cambridge, 2003).
[10] R. Brown and L. Kocarev, Chaos **10**, 344 (2000).
[11] J. A. Acebrón, L. L. Bonilla, C. J. Pérez Vicente, F. Ritort, and R. Spigler, Rev. Mod. Phys. **77**, 137 (2005).

[12]J. Blake and M. Sleigh, Biol. Rev. Cambridge Philos. Soc. **49**, 85 (1974).
[13]S. Nonaka, Y. Tanaka, Y. Okada, S. Takeda, A. Harada, Y. Kanai, M. Kido, and N. Hirokawa, Cell **95**, 829 (1998).
[14]Y. Okada, S. Nonaka, Y. Tanaka, Y. Saijoh, H. Hamada, and N. Hirokawa, Mol. Cell **4**, 459 (1999).
[15]B. Alberts, A. Johnson, J. Lewis, M. Raff, K. Roberts, and P. Walter, *Molecular Biology of the Cell*, 4th ed. (Garland, New York, 2002).
[16]D. Wheatley, Cell Biol. Int. **28**, 75 (2004).
[17]N. Hirokawa, Y. Tanaka, Y. Okada, and S. Takeda, Cell **125**, 33 (2006).
[18]S. Vogel, *Life in Moving Fluids: The Physical Biology of Flow* (Princeton University Press, Princeton, 1996).
[19]S. Tamm, T. Sonneborn, and R. Dippell, J. Cell Biol. **64**, 98 (1975).
[20]E. Knight-Jones, Q. J. Microsc. Sci. **95**, 503 (1954).
[21]T. Jahn and J. Votta, Annu. Rev. Fluid Mech. **4**, 93 (1972).
[22]O. Zagoory, A. Braiman, L. Gheber, and Z. Priel, Am. J. Physiol.: Cell Physiol. **280**, C100 (2001).
[23]K. Okamoto and Y. Nakaoka, J. Exp. Biol. **192**, 61 (1994).
[24]P. Lenz and A. Ryskin, Phys. Biol. **3**, 285 (2006).
[25]J. Blake, J. Fluid Mech. **55**, 1 (1972).
[26]N. Liron and S. Mochon, J. Fluid Mech. **75**, 593 (1976).
[27]S. Gueron and N. Liron, Biophys. J. **65**, 499 (1993).
[28]S. Gueron and N. Liron, Biophys. J. **63**, 1045 (1992).
[29]S. Gueron and K. Levit-Gurevich, Proc. R. Soc. London, Ser. B **268**, 599 (2001).
[30]M. Reichert and H. Stark, Eur. Phys. J. E **17**, 493 (2005).
[31]Y. Kuramoto, in *Lecture Notes in Physics No. 30*, edited by H. Araki (Springer, New York, 1975), pp. 420–422.
[32]Y. Kuramoto and I. Nishikawa, J. Stat. Phys. **49**, 569 (1987).
[33]H. Sakaguchi, S. Shinomoto, and Y. Kuramoto, Prog. Theor. Phys. **77**, 1005 (1987).
[34]S. Strogatz and R. Mirollo, Physica D **31**, 143 (1988).
[35]S. Strogatz and R. Mirollo, J. Phys. A **21**, 699 (1988).
[36]H. Daido, Phys. Rev. Lett. **77**, 1406 (1996).
[37]H. Daido, Physica D **91**, 24 (1996).
[38]H. Daido, Phys. Rev. Lett. **61**, 231 (1988).
[39]H. Sakaguchi, S. Shinomoto, and Y. Kuramoto, Prog. Theor. Phys. **79**, 1069 (1988).
[40]Y. Okada, S. Takeda, Y. Tanaka, J. Belmonte, and N. Hirokawa, Cell **121**, 633 (2005).
[41]J. Cartwright, O. Piro, and I. Tuval, Proc. Natl. Acad. Sci. U.S.A. **101**, 7234 (2004).
[42]C. Brennen and H. Winet, Annu. Rev. Fluid Mech. **9**, 339 (1977).
[43]S. Camalet and F. Jülicher, New J. Phys. **2**, 24.1 (2000).
[44]I. Riedel-Kruse, A. Hilfinger, J. Howard, and F. Jülicher, HFSP J. **1**, 192 (2007).
[45]P. Lenz, J. Joanny, F. Jülicher, and J. Prost, Phys. Rev. Lett. **91**, 108104 (2003).
[46]P. Lenz, J. Joanny, F. Jülicher, and J. Prost, Eur. Phys. J. E **13**, 379 (2004).
[47]L. Landau and E. Lifshitz, *Hydrodynamics* (Pergamon, New York, 1959).
[48]M. Mehta, *Matrix Theory* (Hindustan, Delhi, 1989).
[49]W. Wang and J. Slotine, Biol. Cybern. **92**, 38 (2005).
[50]Y. Kim and R. Netz, Phys. Rev. Lett. **96**, 158101 (2006).
[51]Alternatively, the notions full, identical, in-phase, out-of phase, and antiphase synchronization are sometimes used (Ref. 9).